Three-Dimensional Culture of Melanoma Cells Profoundly Affects Gene Expression Profile: A High Density Oligonucleotide Array Study

SOURABH GHOSH,[1] GIULIO C. SPAGNOLI,[1] IVAN MARTIN,[1] SABINE PLOEGERT,[1] PHILIPPE DEMOUGIN,[2] MICHAEL HEBERER,[1] AND ANCA RESCHNER[1]*

[1]*Institut für Chirurgische Forschung und Spitalmanagement (ICFS) and Departement Forschung, University of Basel, Basel, Switzerland*
[2]*Biocenter/Pharmacenter, University of Basel, Basel, Switzerland*

Growth in three-dimensional (3D) architectures has been suggested to play an important role in tumor expansion and in the resistance of cancers to treatment with drugs or cytokines or irradiation. To obtain an insight into underlying molecular mechanisms, we addressed gene expression profiles of NA8 melanoma cells cultured in bidimensional monolayers (2D) or in 3D multicellular tumor spheroids (MCTS). MCTS containing 10-30,000 cells were generated upon overnight culture in poly-Hydroxyethylmethacrylate (polyHEMA) coated plates. Kinetics of cell proliferation in MCTS was significantly slower than in monolayer cultures. Following long-term culture (>10 days), however, MCTS showed highly compact and organised cell growth in outer layers, with necrotic cores. Oligonucleotide microarray analysis of the expression of over 20,000 genes was performed on cells cultured in standard 2D, in the presence of collagen as model of extracellular matrix (ECM), or in MCTS. Gene expression profiles of cells cultured in 2D in the presence or absence of ECM were highly similar, with ≥threefold differences limited to five genes. In contrast, culture in MCTS resulted in the significant, ≥threefold, upregulation of the expression of >100 transcripts while 73 were ≥threefold downregulated. In particular, genes encoding CXCL1, 2, and 3 (GRO-α, -β, and γ), IL-8, CCL20 (MIP-3α), and Angiopoietin-like 4 were significantly upregulated, whereas basic FGF and CD49d encoding genes were significantly downregulated. Oligonucleotide chip data were validated at the gene and protein level by quantitative real-time PCR, ELISA, and cell surface staining assays. Taken together, our data indicate that structural modifications of the architecture of tumor cell cultures result in a significant upregulation of the expression of a number of genes previously shown to play a role in melanoma progression and metastatic process. J. Cell. Physiol. 204: 522–531, 2005. © 2005 Wiley-Liss, Inc.

Experimental models indicate that tumor cells in suspension, regardless of their numbers, are frequently unable to produce life threatening cancer outgrowth, as opposed to solid tumor fragments (Ochsenbein et al., 2001), while being able to induce specific immune responses. Thus, proliferation in structured architectures appears to represent a pre-requisite for cancer development. Therefore, development of three-dimensional (3D) models of neoplastic cell culture may represent a technological approach of potentially high clinical relevance.

Indeed, cells cultured in 3D conditions have been shown to be endowed with specific characteristics, including resistance to apoptosis or to the cytotoxic activity of specific T-cells "in vitro" (Sutherland, 1988; Desoize and Jardillier, 2000; Dangles et al., 2002; Weaver et al., 2002; Dangles-Marie et al., 2003). Notably, multicellular tumor spheroids (MCTS) display drug and radiation resistance features closely matching those frequently detectable "in vivo" (Desoize and Jardillier, 2000).

Taken together, these studies suggest that in tumor cells growing in structured architectures the preferential expression of specific constellations of genes might occur.

In order to obtain insights into similarities and differences between tumor cells growing in physically different microenviroments, here we analyzed gene expression profiles of melanoma cells (Certa et al., 2001) cultured in standard 2D conditions or as MCTS.

MATERIALS AND METHODS

Cell cultures

NA8 cell line was derived from a metastatic melanoma and has widely been used in tumor immunology studies in the recent past (Gervois et al., 1996; Oertli et al., 2002; Zajac et al., 2003). It is HLA-A0201+ but fails to express typical differentiation or cancer/testis (C/T) tumor-associated antigens (TAA) (Renkvist et al., 2001). NA8 cells were routinely passaged in conventional monolayer cultures in DMEM supplemented with Kanamycin, glutamin, non-essential amino acids, sodium pyruvate, HEPES buffer, and 10% heat-inactivated FCS (all from Gibco, Paisley, Scotland), thereafter referred to as complete medium. When indicated, cells were also cultured in dishes previously coated (2 h at 37°C) with a 50 μg/ml solution of purified collagen (Vitrogen, Palo Alto CA) in PBS. MCTS were prepared in plastic culture plates following coating with a 50 μg/ml poly-(2-hydroxyethyl methacrylate, polyHEMA, Sigma, St. Louis, MO) solution, preventing cell binding, as described (Folkman and Moscona, 1978). Cell proliferation was measured by the Alamar Blue assay (Hamid et al., 2004).

Gene expression profiling

Na-8 cells were harvested by trypsinization after 3 days cultures according to the different protocols indicated. Total RNA was extracted using Qiagen Rneasy® Mini Kit (Qiagen, Basel, Switzerland) and its integrity was monitored using Agilent 2100 Bioanalyzer (Ambion, Austin TX). Ten micrograms of RNA from each sample were reverse transcribed and

Contract grant sponsor: Swiss National Science Foundation; Contract grant sponsor: Swiss Bridge Foundation.

*Correspondence to: Anca Reschner, ICFS, Lab. 401, ZLF, 20, Hebelstrasse, 4031, Basel, Switzerland.
E-mail: areschner@uhbs.ch

Received 27 September 2004; Accepted 29 November 2004

DOI: 10.1002/jcp.20320

labeled by using commercial kits according to the suppliers' instructions (MEGAscript T7, Ambion, Austin TX; Bio-11-CTP and Bio-16-UTP, Enzo Biochem, NY). Biotinylated cRNA was then fragmented by treatment at 94°C for 35 min in 40 mM TRIS-acetate, pH 8.1, 100 mM potassium acetate, and 30 mM magnesium acetate and hybridized to human oligonucleotide array HG-U-133A (Affymetrix, Santa Clara CA). Two separate hybridizations were performed for each sample under investigation. Raw data were collected using a confocal laser scanner, and pixel levels were analyzed using commercial software (Gene Spring Version 1.6, Silicon Genetics, Redwood City, CA). For each hybridization, two separate data readings were performed.

Histology and immunohistochemistry

Tumor spheroids were fixed in 4% formaldehyde, washed in PBS, and embedded in paraffin. Sections were stained with hematoxylin and eosin. BrdU staining was performed on fresh frozen MCTS sections, following endogenous peroxidase blocking by incubation with hydrogen peroxide, by taking advantage of a reagent kit (Pharmingen, San Diego, CA), according to the instructions of the supplier. In specific experiments, slides were incubated in the presence of an anti-human IL-8 monoclonal antibody (BD Biosciences Pharmingen, San Diego, CA) for 4 h and specific staining was detected by adding a biotinylated secondary antibody, avidin-HRP, and

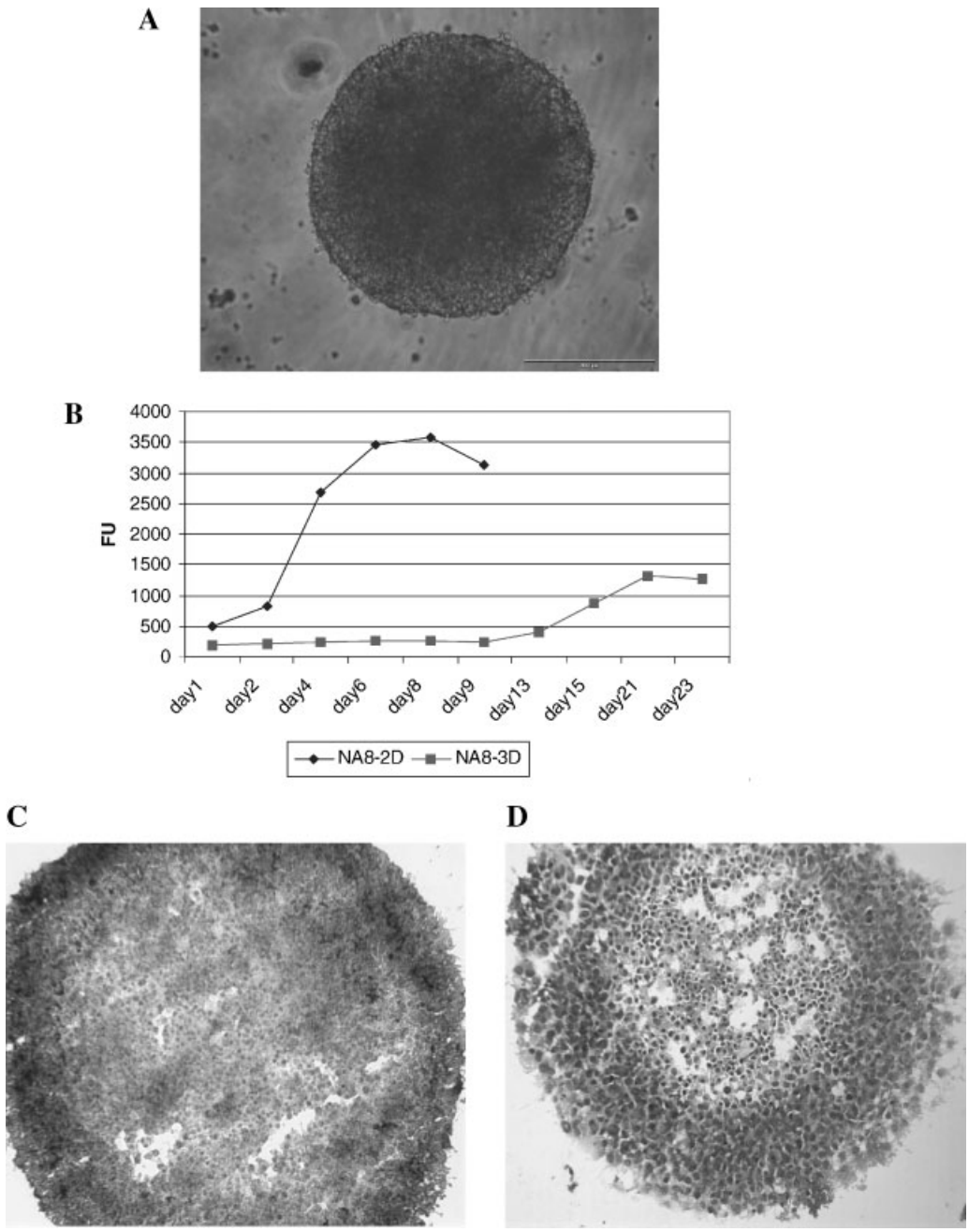

Fig. 1. Generation and characterization of multicellular tumor spheroids of NA8 cells. NA8 cells cultured o/n on polyHema coated plates give rise to the formation of multicellular tumor spheroids (MCTS, part A). Alamar blue cell proliferation assays (part B) show distinct kinetics for cells cultured in monolayers or MCTS. BrdU staining (part C) indicates that while cells located in the center of MCTS are prevailingly in quiescent state, those in outer layers are actively cycling. Prolonged culture (>10 days) results in apoptosis of cells sitting in the inner MCTS layers, resulting in the formation of hollow centers (part D).

3,3′-diaminobenzidine hydrochloride. In all cases, slides were counterstained with hematoxylin.

Real-time RT-PCR

NA-8 cells cultured in 2D or as MCTS were collected at the indicated time points and washed in PBS. Total RNA was extracted using the RNeasy® Mini Kit Protocol (Qiagen, Basel, Switzerland) and treated with deoxyribonuclease I (DNase I) (Invitrogen, Carlsbad, CA). Real-time quantitative RT-PCR assays were conducted on a ABI prism™ 7700 sequence detection system, using TaqMan® One Step PCR Master Mix Reagents Kit (Master Mix without UNG, Multiscribe™ and RNase Inhibitor Mix, Applied Biosystems, Branchburg, NJ).

The oligonucleotide primers and the Taq Man probe for GAPDH were designed using the Primer Express software (Perkin Elmer Applied Biosystems, Inc., Foster City, CA) and sequences from the NCBI gene bank. The primers and probes for CXCL1 (GRO alpha), CXCL8 (IL-8), and CCL20 (MIP-3alpha) were purchased as Assays on Demand, Gene Expression Products (Perkin Elmer Applied Biosystems, Inc., Foster City, CA).

To quantify gene expression in each sample, we used the comparative threshold cycle (Ct) method (Primer Express software, Applied Biosystem, Foster City, CA). Normalization of gene expression was performed by using GAPDH as reference gene, and data were expressed as ratio to a reference sample, namely to cells cultured in standard monolayers.

Protein detection by ELISA

CXCL1, CCL20, and IL-8 secretion was tested by quantitative ELISA assays (sensitivity: $\geq$30 pg/ml) in supernatants from NA-8 monolayer cultures or MCTS sampled at different time points. Antibody pairs and standards for CXCL1 were from R&D Systems (Abingdon, Great Britain), whereas CCL20 and IL-8 ELISA sets were obtained from Becton Dickinson Bioscience Pharmingen, San Diego, CA. All samples were measured in duplicates.

Flow cytometry

NA-8 cells cultured in 2D were collected by trypsinization on day 3. Accordingly, MCTS obtained after 3 days of culture on polyHEMA treated plasticware were centrifuged and pellets were disrupted by Trypsin-EDTA (Gibco, Paisley, Great Britain) treatment for 30 min at 37°C. Phenotypes of NA-8 cells cultured in 2D or 3D were evaluated by surface staining using fluorochrome conjugated mouse monoclonal antibodies recognizing the indicated determinants. Samples were analyzed on a FACSCalibur (Becton Dickinson, San Jose, CA) using propidium iodide (PI) to exclude dead cells.

Statistical analysis

One-way ANOVA tests were performed for gene lists filtered on fold change in the log-of-ratio mode of experimental interpretation (Gene Spring 6 software, Silicon Genetics, Redwood City, CA). Duplicates of each experimental group were compared. The parametric Welch *t*-test was used within the study with a cut-off *P*-value of 0.05.

RESULTS

Morphological characterization and growth pattern of NA8 melanoma cell spheroids

NA8 cells were routinely maintained in 2D cultures in complete medium. However, treatment of culture trays with polyHEMA (Folkman and Moscona, 1978), preventing cell attachment, gave rise within 24 h to the formation of MCTS structures. Each MCTS, displaying 400–500-μm diameter, contained between 10,000 and 30,000 cells (Fig. 1A). NA8 cell proliferation in 2D cultures was reaching a plateau within 7 days, whereas, in contrast, no major increases in cell numbers were detectable in MCTS for the first 2 weeks of culture, but they could only be observed at later time points (Fig. 1B). BrdU staining indicated that while cells in the outer MCTS layers were entering cell cycle, those of inner layers were mostly quiescent (Fig. 1C). Furthermore, upon prolonged culture (>10 days), HE staining showed necrotic cores within MCTS soon resulting in hollow centers with large, compact cells being typically detectable in the periphery (Fig. 1D).

Gene expression profiles of NA8 cells cultured in 2D and in spheroids

The expression of specific sets of genes has previously been shown to be modulated by cell culture architecture (Dangles et al., 2002), possibly also in relation to signals effectively transduced upon interaction of adhesion molecules with their counter receptors (Cavallaro and Christofori, 2004). Prompted by these studies, we addressed thorough gene profiling in NA8 cells cultured in standard 2D conditions, in the presence of extracellular matrix (ECM) or in MCTS, by taking advantage of high-density oligonucleotide arrays allowing the analysis of over 20,000 expressed genes. As ECM model, we

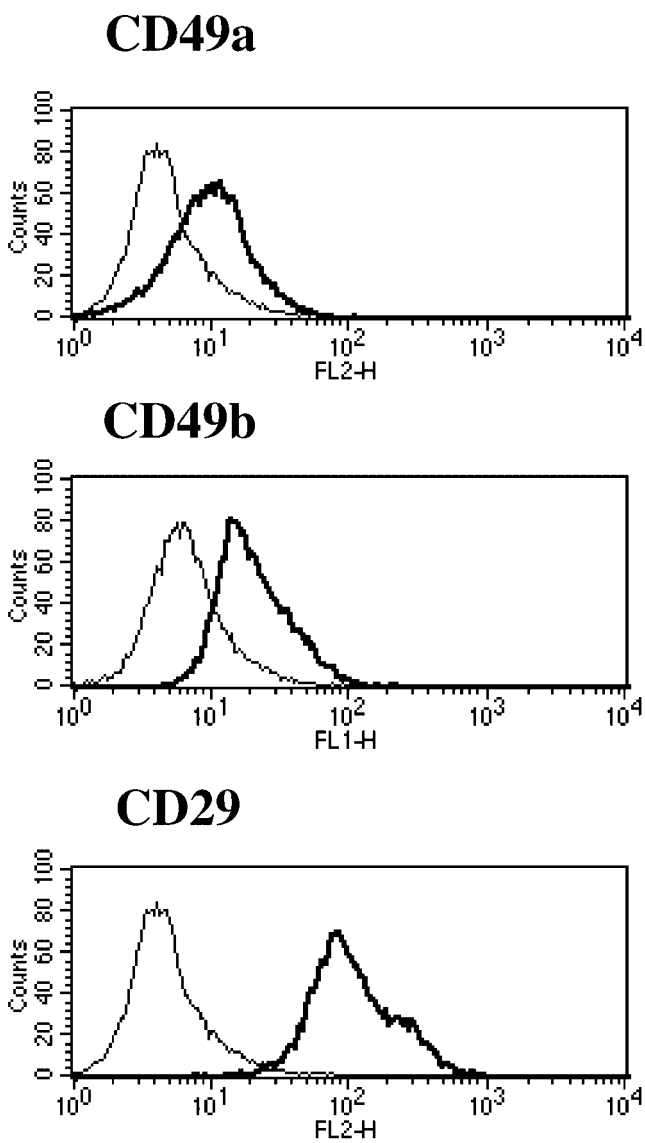

Fig. 2. Expression of receptors for collagen in NA8 cells. NA8 cells cultured in standard monolayers were trypsinized and stained with monoclonal antibodies specific for α1, α2, and β1 (CD49a, CD49b, and CD29, respectively), integrin chains.

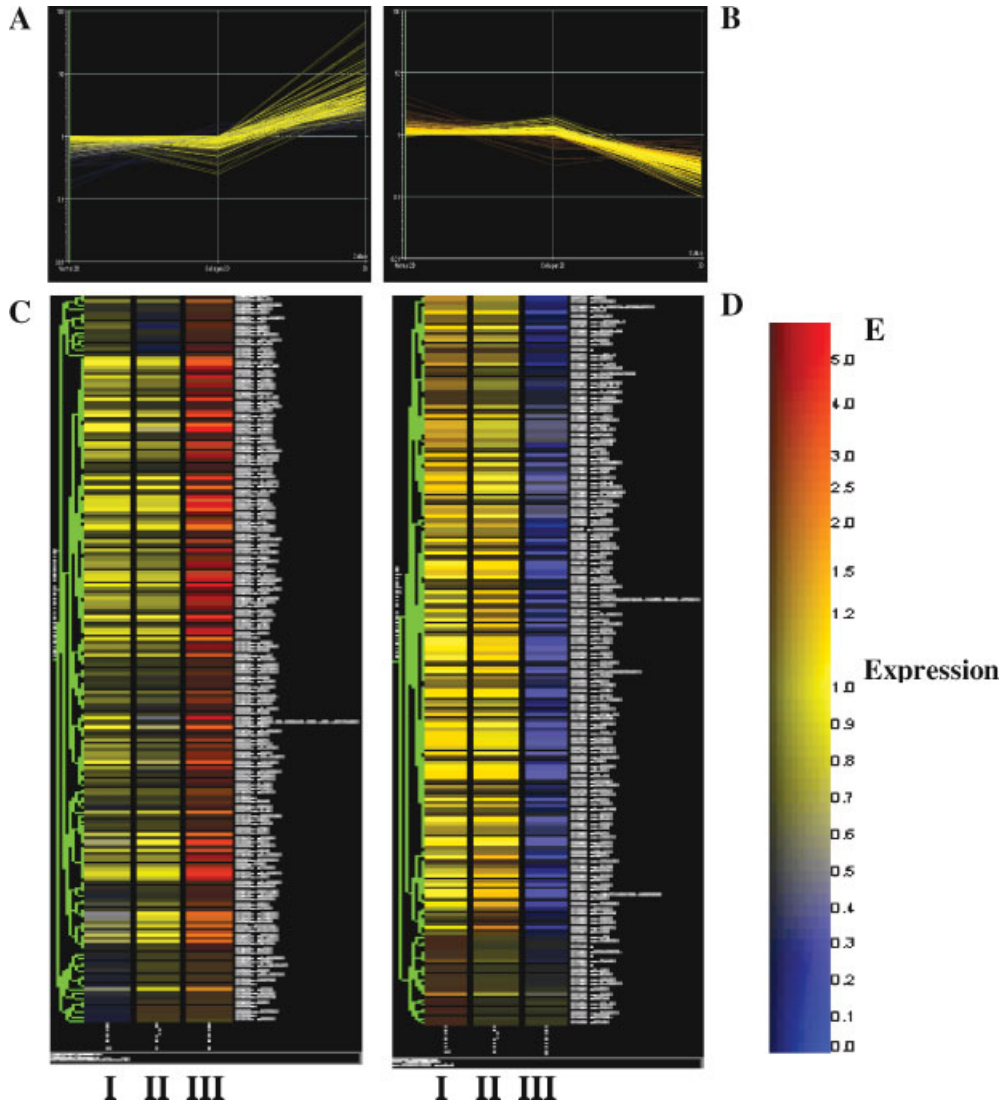

Fig. 3. Modulation of gene expression in NA8 cells cultured in 2D or MCTS. NA8 melanoma cells were cultured in standard monolayers (I), in 2D in the presence of solid phase bound collagen (II) or in MCTS (III). Parts A and B refer to genes significantly up- or downregulated, respectively, in either of these culture conditions. The extent of the up- or downregulation of each gene is presented in parts C and D, respectively, according to the color scale shown in part E.

chose collagen since NA8 cells express both $\alpha 1\beta 1$ and $\alpha 2\beta 1$ integrin receptors (Fig. 2).

Over 11,000 genes were found to be expressed in NA8 cells. Cells cultured in monolayers, irrespective of the presence of ECM, showed remarkably similar gene expression patterns (Fig. 3), with statistically significant differences (see above) being limited to five genes (Table 1). In particular, a downregulation (fivefold) of Hsp 40 encoding gene was observed in cells cultured in the presence of collagen.

In contrast, cells cultured in MCTS displayed significant modulation in the expression of a number of genes as compared to their monolayer counterparts. Indeed, 106 genes showed evidence of upregulation and 73

TABLE 1. Modulation of gene expression in NA8 monolayers in the presence or absence of collagen coating

Common name	Genbank	Description	*P*-value	Fold change
Genes upregulated in 2D NA8 cultures in the presence of collagen (as compared to monolayer NA8 cells)				
INHBA	NM_002192	Inhibin, beta A (activin A, activin AB alpha polypeptide)	0.03785189	3.23
Genes downregulated in 2D NA8 cultures in the presence of collagen (as compared to monolayer NA8 cells)				
LRRC19	NM_022901	Leucine-rich repeat containing 19	0.04999528	3.36
	AK025191	*Homo sapiens* cDNA: FLJ21538 fis, clone COL06151	0.02274983	4.49
DNAJC6	NM_014787	DnaJ (Hsp40) homolog, subfamily C, member 6	0.02692304	5.05
PF4V1	NM_002620	Platelet factor 4 variant 1	0.04518665	10.36

NA8 cells were cultured in monolayers in the presence or absence of collagen coating for 3 days. Total cellular RNA was then extracted, reverse transcribed, and labeled as described in Materials and Methods prior to hybridization to oligonucleotide chips. Only genes displaying a $\geq$threefold up- or downregulation (fold change) in either culture conditions are reported. Statistical significance ($P < 0.05$) refers to duplicate readings of data obtained from two distinct hybridization experiments.

TABLE 2. Modulation of gene expression in NA8 cells cultured in MCTS, as compared to standard monolayers

Common name	Genbank	Description	*P*-value	Fold change
Genes upregulated in MCTS as compared to monolayer NA8 cells				
CCL20	NM_004591	Chemokine (C-C motif) ligand 20	0.00269	75.29
IL8	NM_000584	Interleukin 8	0	67.9
IL8	AF043337	*Homo sapiens* interleukin 8 C-terminal variant (IL8) mRNA, complete cds.	0.0008	59.76
ANGPTL4	NM_016109	Angiopoietin-like 4	0.00139	34.37
SLC2A3	NM_006931	Solute carrier family 2 (facilitated glucose transporter), member 3	0.00021	33.63
CA9	NM_001216	Carbonic anhydrase IX	0.00118	31.38
NDRG1	NM_006096	N-myc downstream regulated gene 1	0.01835	28.71
STC1	NM_003155	Stanniocalcin 1	0.00178	23.63
ITPR1	NM_002222	Inositol 1,4,5-triphosphate receptor, type 1	0.0053	22.76
ADFP	BC005127	Adipose differentiation-related protein	0.02111	17.27
LOX	L16895	Human lysyl oxidase (LOX) gene, exon 7	0.03525	16.23
CXCL2	M57731	Chemokine (C-X-C motif) ligand 2	0.01738	15.90
LOX	BE503425	Lysyl oxidase	0.00862	14.45
ISG20	NM_002201	Interferon-stimulated gene 20kDa	0.02148	14.11
ADM	NM_001124	Adrenomedullin	0.00801	13.36
C10orf10	AI302100	Chromosome 10 open reading frame 10	0.0484	12.94
TBC1D3	AL136860	TBC1 domain family, member 3	0.04100	12.69
SLC2A3	NM_006931	Solute carrier family 2 (facilitated glucose transporter), member 3	0.0037	12.58
CXCL1	NM_001511	Chemokine (C-X-C motif) ligand 1 (melanoma growth stimulating activity, alpha)	0.03033	10.14
TNFAIP3	NM_006290	Tumor necrosis factor, alpha-induced protein 3	0.03686	9.38
DUSP6	BC003143	Dual specificity phosphatase 6	0.00856	9.21
SPAG4	NM_003116	Sperm associated antigen 4	0.01191	9.06
ANXA10	AF196478	Annexin A10	0.03017	8.89
MAFF	AL021977	Human DNA sequence from clone CTA-447C4 on chromosome 22q12.2-13.2, complete sequence.	0.04029	8.83
BHLHB2	BG326045	Basic helix-loop-helix domain containing, class B, 2	0.01762	8.49
SAT	BE971383	Spermidine/spermine N1-acetyltransferase	0.01839	8.35
SOD2	AL050388	Superoxide dismutase 2, mitochondrial	0.04224	8.11
RIS1	BF062629	Ras-induced senescence 1	0.02817	7.7
STC1	AI300520	Stanniocalcin 1	0.02172	7.54
NT5E	NM_002526	5′-nucleotidase, ecto (CD73)	0.01339	7.50
C1orf29	NM_006820	Chromosome 1 open reading frame 29	0.04604	7.29
HIG2	NM_013332	Hypoxia-inducible protein 2	0.02166	7.02
RNASE4	AI761728	Ribonuclease, RNase A family, 4	0.01996	6.76
FLJ10134	NM_018004	Hypothetical protein FLJ10134	0.00496	6.63
BNIP3	NM_004052	BCL2/adenovirus E1B 19kDa interacting protein 3	0.01031	6.56
SLC2A14	AL110298	Solute carrier family 2 (facilitated glucose transporter), member 14	0.01999	6.37
IER3	NM_003897	Immediate early response 3	0.02379	6.34
CXCL3	NM_002090	Chemokine (C-X-C motif) ligand 3	0.00576	6.17
TNFAIP3	AI738896	Tumor necrosis factor, alpha-induced protein 3	0.04375	6.04
ENO2	NM_001975	Enolase 2, (gamma, neuronal)	0.04872	5.99
SOD2	W46388	Superoxide dismutase 2, mitochondrial	0.01667	5.96
STC2	AI435828	Stanniocalcin 2	0.04571	5.69
E2IG5	NM_014367	Growth and transformation-dependent protein	0.03707	5.69
HSPA6	NM_002155	Heat shock 70-kDa protein 6 (HSP70B′)	0.03255	5.49
PPP1R15A	NM_014330	Protein phosphatase 1, regulatory (inhibitor) subunit 15A	0.01399	5.44
MXI1	NM_005962	MAX interacting protein 1	0.00564	5.36
PPP1R3C	N26005	Protein phosphatase 1, regulatory (inhibitor) subunit 3C	0.001	5.32
SLCO4A1	NM_016354	Solute carrier organic anion transporter family, member 4A1	0.02663	5.26
SERPINE1	AL574210	Serine (or cysteine) proteinase inhibitor, clade E (nexin, plasminogen activator inhibitor type 1), member 1	0.04204	5.22
BNIP3	U15174	*Homo sapiens* BCL2/adenovirus E1B 19kD-interacting protein 3 (BNIP3) mRNA, complete cds.	0.00914	5.16
BTG1	AL535380	B-cell translocation gene 1, anti-proliferative	0.03111	5.14
SOD2	BF575213	Superoxide dismutase 2, mitochondrial	0.00027	5.11
IGFBP3	NM_000598	Insulin-like growth factor binding protein 3	0.01595	5.05
CDCP1	NM_022842	CUB domain-containing protein 1	0.04963	5.03
SERPINA3	NM_001085	Serine (or cysteine) proteinase inhibitor, clade A (alpha-1 antiproteinase, antitrypsin), member 3	0.00283	4.72
BHLHB2	NM_003670	Basic helix-loop-helix domain containing, class B, 2	0.03066	4.68
DPYSL4	NM_006426	Dihydropyrimidinase-like 4	0.02427	4.6
MT1H	NM_005951	Metallothionein 1H	0.03048	4.42
SERPINB4	AB046400	Serine (or cysteine) proteinase inhibitor, clade B (ovalbumin), member 4	0.0285	4.39
TFPI2	L27624	Tissue factor pathway inhibitor 2	0.04993	4.38
KIAA1641	NM_025190	KIAA1641 protein	0.03702	4.35
IL1B	NM_000576	Interleukin 1, beta	0.01032	4.22
KIAA0703	AW291664	KIAA0703 gene product	0.02643	4.21
NFIL3	NM_005384	Nuclear factor, interleukin 3 regulated	0.00834	4.21
DIPA	BG251266	Hepatitis delta antigen-interacting protein A	0.00501	4.19
GOLGIN-67	AF204231	Golgin-67	0.03727	4.13
RNU2	BC003629	Synonym: U2; *Homo sapiens* RNA, U2 small nuclear, mRNA (cDNA clone MGC:2854 IMAGE:2987935), complete cds.	0.00908	4.13
INSIG2	AL080184	Insulin induced gene 2	0.00952	4.13
PHLDA1	AA576961	Pleckstrin homology-like domain, family A, member 1	0.03627	4.09
LAMB3	L25541	Laminin, beta 3	0.01549	3.99
DUSP1	NM_004417	Dual specificity phosphatase 1	0.00041	3.99

TABLE 2. (*Continued*)

Common name	Genbank	Description	*P*-value	Fold change
RTP801	NM_019058	HIF-1 responsive RTP801	0.00224	3.92
NFKBIA	AI078167	Nuclear factor of kappa light polypeptide gene enhancer in B-cells inhibitor, alpha	0.04187	3.9
G0S2	NM_015714	Putative lymphocyte G0/G1 switch gene	0.03401	3.9
PLA2G4A	M68874	Phospholipase A2, group IVA (cytosolic, calcium-dependent)	0.01971	3.88
PLAB	AF003934	Prostate differentiation factor	0.01362	3.86
SLC2A14	AA778684	Solute carrier family 2 (facilitated glucose transporter), member 14	0.01172	3.85
MUC1	AI610869	Mucin 1, transmembrane	0.04501	3.84
PDK1	NM_002610	Pyruvate dehydrogenase kinase, isoenzyme 1	0.00676	3.8
BTG1	NM_001731	B-cell translocation gene 1, anti-proliferative	0.02923	3.76
JUN	BG491844	v-jun sarcoma virus 17 oncogene homolog (avian)	0.03386	3.72
GJA1	NM_000165	Gap junction protein, alpha 1, 43 kDa (connexin 43)	0.00254	3.72
LAMA4	NM_002290	Laminin, alpha 4	0.02974	3.71
LIF	NM_002309	Leukemia inhibitory factor (cholinergic differentiation factor)	0.03757	3.63
CLECSF2	BC005254	C-type (calcium dependent, carbohydrate-recognition domain) lectin, superfamily member 2 (activation-induced)	0.04020	3.62
ICAM1	NM_000201	Intercellular adhesion molecule 1 (CD54), human rhinovirus receptor	0.04134	3.58
EFNA1	NM_004428	Ephrin-A1	0.00912	3.57
F11R	AF154005	F11 receptor	0.03130	3.50
MT1L	NM_002450	Metallothionein 1L	0.04294	3.48
TNIP1	NM_006058	TNFAIP3 interacting protein 1	0.0289	3.47
DPYSL4	AW090187	Dihydropyrimidinase-like 4	0.03598	3.4
RELB	NM_006509	v-rel reticuloendotheliosis viral oncogene homolog B, nuclear factor of kappa light polypeptide gene enhancer in B-cells 3 (avian)	0.01863	3.40
IFI27	NM_005532	Interferon, alpha-inducible protein 27	0.01513	3.39
MSH3	NM_002439	mutS homolog 3 (E. coli)	0.04185	3.37
TPBG	NM_006670	Trophoblast glycoprotein	0.0004	3.3
IL1RAP	AF167343	Interleukin 1 receptor accessory protein	0.01481	3.25
OR12D2	NM_013936	Olfactory receptor, family 12, subfamily D, member 2	0.00764	3.24
	AF333388	MT-1H-like protein; mutant as compared to wild-type sequence MT-1H in GenBank Accession Number X64834; *Homo sapiens* metallothionein 1H-like protein mRNA, complete cds.	0.03535	3.23
SERPINB4	U19557	Serine (or cysteine) proteinase inhibitor, clade B (ovalbumin), member 4	0.03171	3.23
ATF3	NM_001674	Activating transcription factor 3	0.00921	3.21
UPK1A	AA548647	Uroplakin 1A	0.02299	3.19
ETS2	AV700891	v-ets erythroblastosis virus E26 oncogene homolog 2 (avian)	0.02611	3.15
ITGA2	NM_002203	Integrin, alpha 2 (CD49B, alpha 2 subunit of VLA-2 receptor)	0.01431	3.08
BNIP3L	AL132665	BCL2/adenovirus E1B 19kDa interacting protein 3-like	0.03174	3.08
IRF7	NM_004030	Interferon regulatory factor 7	0.03687	3.07
PBEF	NM_005746	Pre-B-cell colony-enhancing factor	0.04173	3.05
HAS2	NM_005328	Hyaluronan synthase 2	0.03363	3.05
Genes downregulated in MCTS as compared to monolayer NA8 cells				
C6orf11	BC000388	Chromosome 6 open reading frame 11	0.0018	10.23
KIAA0918	AW449813	KIAA0918 protein	0.0012	10.05
UTX	NM_021140	Ubiquitously transcribed tetratricopeptide repeat gene, X chromosome	0.0353	7.44
SLC25A14; UCP5; BMCP1	AF155810	UCP5SI; alternatively spliced; *Homo sapiens* mitochondrial uncoupling protein 5 short form with insertion mRNA, complete cds; nuclear gene for mitochondrial product	0.0192	6.94
FGF2	NM_002006	Fibroblast growth factor 2 (basic)	0.0296	6.80
FLJ20220	NM_017718	Hypothetical protein FLJ20220	0.0233	6.19
CDC42BPA	NM_003607	CDC42 binding protein kinase alpha (DMPK-like)	0.0277	6.16
MEST	NM_002402	Mesoderm specific transcript homolog (mouse)	0.0099	6.02
OGT	BF001665	O-linked N-acetylglucosamine (GlcNAc) transferase (UDP-N-acetylglucosamine:polypeptide-N-acetylglucosaminyl transferase)	0.0469	5.93
CHN1	BF339445	602038795F1 NCI_CGAP_Brn64 *Homo sapiens* cDNA clone IMAGE:4186582 5′, mRNA sequence.	0.0365	5.70
	AA721025	*Homo sapiens* transcribed sequence with moderate similarity to protein ref:NP_060265.1 (H. sapiens) hypothetical protein FLJ20378 [*Homo sapiens*]	0.0203	5.59
PDE4B	NM_002600	Phosphodiesterase 4B, cAMP-specific (phosphodiesterase E4 dunce homolog, *Drosophila*)	0.0280	5.37
BCMSUNL	AA905286	*Homo sapiens* cDNA FLJ12357 fis, clone MAMMA1002352	0.0453	5.33
KCTD12	AF052169	Potassium channel tetramerisation domain containing 12	0.0049	5.22
FBN2	NM_001999	Fibrillin 2 (congenital contractural arachnodactyly)	0.0105	5.18
HIST1H2BH	NM_003524	Histone 1, H2bh	0.0446	5.07
SMYD5	U50383	SMYD family member 5	0.0091	5.03
LOC92249	AU154785	Hypothetical protein LOC92249	0.0054	5.01
CALD1	AL577531	Caldesmon 1	0.0250	4.95
HIST1H3H	NM_003536	Histone 1, H3h	0.0222	4.88
ATR	U49844	Ataxia telangiectasia and Rad3 related	0.0471	4.72
SCD	AF116616	Predicted protein of HQ0998; *Homo sapiens* PRO0998 mRNA, complete cds.	0.0377	4.60
CXCL5	AK026546	Chemokine (C-X-C motif) ligand 5	0.0279	4.51
ID3	NM_002167	Inhibitor of DNA binding 3, dominant negative helix-loop-helix protein	0.0472	4.50
TIMP2	NM_003255	Tissue inhibitor of metalloproteinase 2	0.0202	4.48
TOP3B	AA581879	*Homo sapiens* hypothetical protein similar to topoisomerase (DNA) III beta (H. sapiens) (LOC129020), mRNA	0.0163	4.44
ZNF434	NM_024340	Synonyms: MGC4179, FLJ20417, FLJ31901; *Homo sapiens* zinc finger protein 434 (ZNF434), mRNA	0.0064	4.30

(*Continued*)

TABLE 2. (*Continued*)

Common name	Genbank	Description	*P*-value	Fold change
KNS2	AA284075	Kinesin 2 60/70kDa	0.0098	4.30
SCD	AB032261	Stearoyl-CoA desaturase (delta-9-desaturase)	0.0163	4.26
CD24	AA761181	nz09g03.s1 NCI_CGAP_GCB1 *Homo sapiens* cDNA clone IMAGE:1287316 3′ similar to gb:M57627 INTERLEUKIN-10 PRECURSOR (HUMAN);, mRNA sequence	0.0477	4.12
TPM1	NM_000366	Tropomyosin 1 (alpha)	0.0058	4.09
RHOBTB3	NM_014899	Rho-related BTB domain containing 3	0.0277	3.99
C14orf1	AC007182		0.0491	3.98
SCD	AA678241	Stearoyl-CoA desaturase (delta-9-desaturase)	0.0273	3.97
SEC23B	AL121900		0.0413	3.97
DCN	AF138302	Decorin	0.0146	3.83
IDE	N22903	Insulin-degrading enzyme	0.0079	3.82
MYL9	NM_006097	Myosin, light polypeptide 9, regulatory	0.0325	3.82
NaGLT1; KIAA1919; MGC33953	AK000168	*Homo sapiens* cDNA FLJ20161 fis, clone COL09252, highly similar to L33930 *Homo sapiens* CD24 signal transducer mRNA	0.0032	3.76
MEP50	BF975273	MEP50 protein	0.0369	3.76
TAGLN	NM_003186	Transgelin	0.0452	3.75
SFRS1	M72709		0.0164	3.72
BMP2K	AW504018	BMP2 inducible kinase	0.0376	3.71
G6PD	NM_000402	Glucose-6-phosphate dehydrogenase	0.0273	3.65
NRG1	NM_013959	Neuregulin 1	0.0471	3.60
GCLM	NM_002061	Glutamate-cysteine ligase, modifier subunit	0.0180	3.57
TACSTD2; M1S1; EGP-1; GA733; TROP2; GA733-1	J04152	GA733-1 protein precursor; Human gastrointestinal tumor-associated antigen GA733-1 protein gene, complete cds, clone 05516	0.0069	3.50
NQO1	NM_000903	NAD(P)H dehydrogenase, quinone 1	0.0346	3.44
NOL6	NM_022917	Nucleolar protein family 6 (RNA-associated)	0.0403	3.39
FLJ21125	NM_024627	Hypothetical protein FLJ21125	0.0238	3.39
	AL358975		0.0087	3.31
ALDH3A2	L47162	Aldehyde dehydrogenase 3 family, member A2	0.0003	3.30
FZD2	L37882	Frizzled homolog 2 (Drosophila)	0.0256	3.27
LDLR	AI861942	Low-density lipoprotein receptor (familial hypercholesterolemia)	0.0496	3.27
NICE-4	NM_014847	NICE-4 protein	0.0110	3.23
CDC42BPB	NM_006035	CDC42 binding protein kinase beta (DMPK-like)	0.0380	3.23
JAG1	U77914	Jagged 1 (Alagille syndrome)	0.0274	3.21
TPM1	M19267	Tropomyosin; human tropomyosin mRNA, complete cds.	0.0004	3.21
HSPA1A	U56725	Alternatively spliced mRNA corresponding to the rodent testis enriched heat shock protein 70 kDa family member; Human heat shock protein mRNA, complete cds.	0.0455	3.20
CPA4	NM_016352	Carboxypeptidase A4	0.0216	3.20
FLJ20010	NM_019021	Hypothetical protein FLJ20010	0.0259	3.18
CD24	M58664	CD24 antigen (small cell lung carcinoma cluster 4 antigen)	0.0294	3.17
PAPSS2	AW299958	3′-Phosphoadenosine 5′-phosphosulfate synthase 2	0.0051	3.17
GPC1	AI354864	Glypican 1	0.0498	3.17
GTF3C1	NM_001520	General transcription factor IIIC, polypeptide 1, alpha 220kDa	0.0485	3.14
RBM14	NM_006328	RNA binding motif protein 14	0.0139	3.14
NFATC3	U85430	Nuclear factor of activated T-cells, cytoplasmic, calcineurin-dependent 3	0.0221	3.13
ACTBP9	D50604	Human beta-cytoplasmic actin (ACTBP9) pseudogene	0.0183	3.09
RBM5	NM_005778	RNA binding motif protein 5	0.0413	3.09
VCP	AF100752	Valosin-containing protein	0.0009	3.09
ACTN4; FSGS; FSGS1	U48734	Human non-muscle alpha-actinin mRNA, complete cds.	0.0416	3.08
ITGA4	L12002	Integrin, alpha 4 (antigen CD49D, alpha 4 subunit of VLA-4 receptor)	0.0044	3.08
LSS	AW084510	Lanosterol synthase (2,3-oxidosqualene-lanosterol cyclase)	0.0001	3.06
LAPTM4B	NM_018407	Lysosomal associated protein transmembrane 4 beta	0.0081	3.03

NA8 cells were cultured in MCTS (3D) or in 2D monolayers for 3 days. Total cellular RNA was reverse transcribed, labeled, and hybridized to oligonucleotide chips. Only genes displaying a ≥threefold up- or downregulation (fold change) in either culture conditions are reported. Statistical significance ($P < 0.05$) refers to data obtained from duplicate readings of two distinct hybridization assays.

of downregulation (Fig. 3, parts A, C and parts B, D, respectively). Table 2 reports the names of the genes of interest and their change factors depending on the architecture of NA8 cell culture.

In particular, a significant upregulation of the expression of genes encoding a number of chemokines, including CXCL1, CXCL2, and CXCL3, (GRO-α, -β, and -γ, 10-, 15-, and 6-fold, respectively), IL-8 (67-fold), and CCL20 (75-fold) was detectable in MCTS, as compared to cells cultured in 2D.

The expression of genes encoding pro-angiogenic factors or adhesion molecules, such as angiopoietin-like 4 (34-fold) or hypoxia inducible protein 2 (HIG2, 7-fold) and CD54 (ICAM1, 3.5-fold), was also found to be significantly upregulated in MCTS in comparison with cells growing in monolayers. Interestingly, however, the expression of the genes encoding α4 integrin subunit and fibroblast growth factor 2 (FGF2) was found to be significantly downregulated (3- and 6.8-fold, respectively) in these same conditions.

Validation of differential gene expression

Large gene expression databases require validation at the gene and protein level. Real-time, quantitative RT-PCR confirmed the upregulation of CXCL1 (GRO-α), gene expression in cells sampled after 3-day culture in MCTS, as compared with cells growing in monolayers (Fig. 4, part A). We were then interested in investigating whether the upregulation of CXCL1 gene reflected transient events, merely related to MCTS formation or more durable modifications of NA8 gene expression profile. Indeed, CXCL1 gene upregulation,

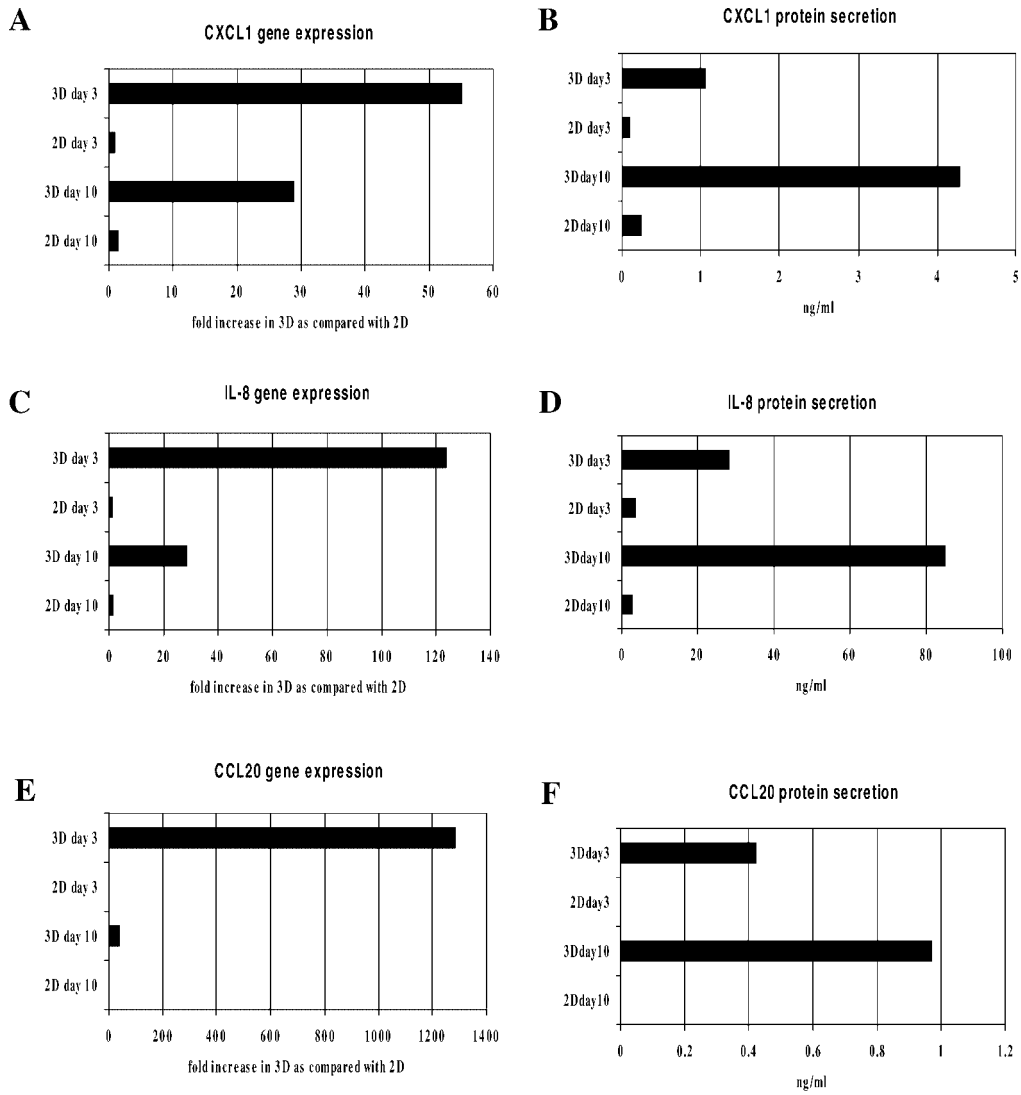

Fig. 4. Chemokine gene expression and protein secretion in NA8 cells cultured in monolayers and MCTS. NA8 cells were cultured for 3 or 10 days in standard monolayer cultures (2D) or in MCTS (3D). Total cellular RNA was then extracted and CXCL1 (GRO-α), IL-8, and CCL20 (MIP-3α) gene expression was evaluated comparatively in cells cultured in 2D or in 3D at the indicated time points by quantitative real-time RT-PCR (parts A, C, and E, respectively). Data are expressed as fold increases of specific gene expression in samples from 3D MCTS cultures as compared to the corresponding samples from 2D cultures at the indicated time points. Secretion of the specific gene products was measured by ELISA in supernatants of cultures containing 3×10^5 cells/ml concomitantly collected (parts B, D, and E, respectively). Standard deviations, never exceeding 10% of the values reported, were omitted.

although declining, was still observed at 10 days after the initiation of cultures. Accordingly, secretion of this chemokine was significantly increased in cells cultured in MCTS as compared to their monolayer cultured counterparts at both 3 and 10 days of culture (Fig. 4, part B).

Similarly, increased IL-8 gene expression, as detected by oligonucleotide array hybridization of cRNA from 3 days MCTS in comparison to 2D cultures, could be confirmed by real-time RT-PCR at 3 and, to a lower extent, at 10 days. Accordingly, significant increases in protein secretion were also observed (Fig. 4, parts C and D). Most conspicuously, massive IL-8 secretion, exceeding 80 ng/ml, was detected in supernatants of NA-8 cells cultured for 10 days in MCTS. Interestingly, immunohistochemical studies (Fig. 5) revealed that IL-8 specific staining was detectable in MCTS, with a preferential localization in inner cell layers.

The marked increase in the expression of CCL20 (MIP-3α) gene in cells cultured in MCTS, as compared to monolayers, detected upon oligonucleotide chip hybridization, was also confirmed by real-time RT-PCR. ELISA assays showed a significant increase in CCL20 protein secretion from MCTS at 3 and 10 days as compared to cells cultured in 2D for the same time, whereas specific gene expression declined in 10 days MCTS (Fig. 4, parts E and F).

On the other hand, regarding adhesion molecules, the genes encoding CD49d and CD54 were shown to be significantly down- and upregulated, respectively, in cells cultured in MCTS as compared to monolayers, by oligonucleotide chip analysis. Cells cultured with different architectures were trypsinized and stained with specific mAb. As reported in Figure 6, flow-cytometry surface expression data were found to be consistent with gene expression results.

Taken together, these data strongly support the integrity of the gene profiling methods adopted in the current study.

DISCUSSION

Three-dimsensional (3D) culture models have been explored in the past decade, aiming at the development

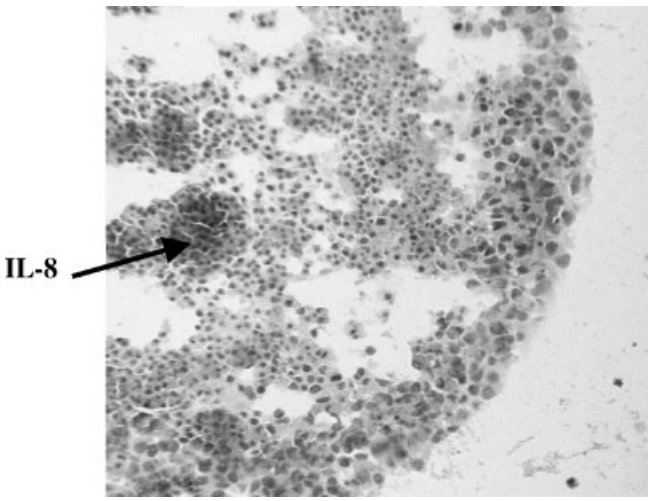

Fig. 5. Immunohistochemical detection of IL-8 in MCTS. Na8 cells were cultured for 10 days in MCTS. Spheroids were then fixed, processed as detailed in Materials and Methods, and incubated in the presence of a monoclonal antibody recognizing IL-8. Specific staining is preferentially detectable in the inner layers of MCTS.

of "in vitro" assays of radio or chemoresistence more closely related to "in vivo" conditions than standard monolayer cultures (Sutherland, 1988). In particular, multicellular tumor spheroids (MTCS) have been suggested to closely reflect early events of avascular tumor growth (Hauptmann et al., 1998; Desoize and Jardillier, 2000). Indeed, MCTS resemble "in vivo" tumors in their capacity to develop necrotic areas far from nutrient and oxygen supplies. Furthermore, MCTS are also similar to solid tumors in their growth dynamics, fitting the Gompertz equation, traditionally used to describe the size limiting growth of tumors (Bajzer et al., 1997; Chignola et al., 2000).

Different methods may be used to obtain MCTS (Kelm et al., 2003). Easy formation in a short time, homogeneous size distribution and reproducibility represent essential requirements. However, extensive manipulation or binding to artificial substrates or beads might result in alterations of the original characteristics of the cells under investigation (Santini et al., 1999). Therefore, in this work, we chose to generate MCTS by merely preventing cell attachment on culture plasticware by polyHEMA (Folkman and Moscona, 1978). In these conditions, spheroid formation was rapidly obtained from NA8 melanoma cells. These MCTS presented features largely overlapping with those of published cell models, regarding slow proliferation (Görlach et al., 1994) and formation of necrotic/hollow cores following long-term culture (Hauptmann et al., 1998). We have comparatively assessed gene expression in identical cells cultured in MCTS or in conventional monolayers. The data presented here provide the first large-scale gene profile analysis of tumor cells cultured in different architectures.

Interestingly, although NA8 cells expressed receptor integrins, $\alpha1\beta1$ and $\alpha2\beta1$, culture on collagen-coated plasticware did not appear to result in major alterations of their gene expression profile. In contrast, culture in MCTS determined profound modifications of the gene expression pattern of NA8 cells, as compared with their counterparts cultured in 2D.

Most remarkably, at least two genes whose products, CXCL1 (GRO-α) and IL-8, have been shown to play a relevant role in melanoma progression and metastatic process (Balentien et al., 1991; Koch et al., 1992; Singh et al., 1994; Luan et al., 1997; Bar-Eli, 1999) were found to be significantly upregulated in cells cultured in MCTS as opposed to monolayers. Massive increases in the

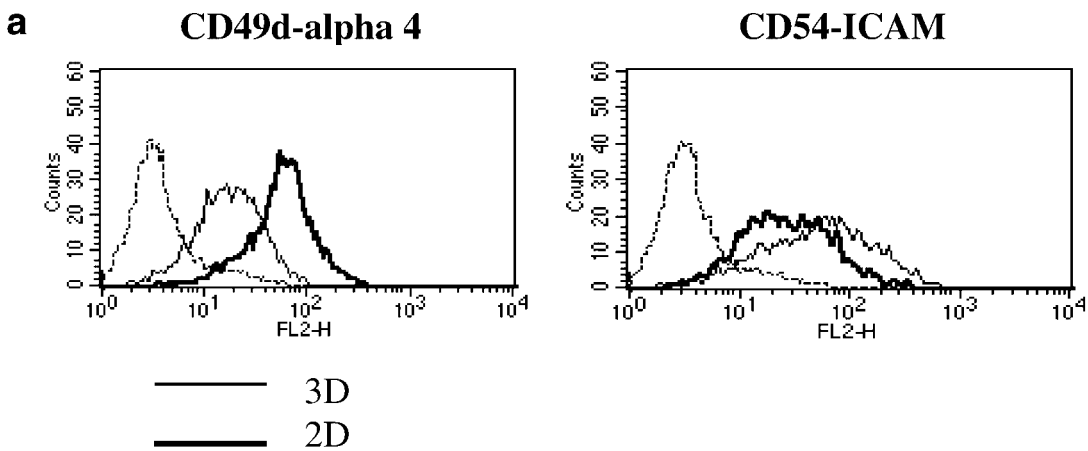

b

Gene	Expression [a]	MFI 2D [b]	MFI MCTS
CD49d	3 fold downregulated in MTCS	57.3	15.4
CD54/ICAM1	3.5 fold upregulated in MTCS	31.1	76.6

Fig. 6. Modulation of adhesion molecule expression in NA8 cells cultured in monolayers or MCTS. NA8 cells were cultured for 3 days in standard monolayer cultures (2D) or in MCTS (3D). They were subsequently trypsinized and stained with CD49d or CD54 specific monoclonal antibodies or isotype matched controls. **a**: Data refer to modulation of gene expression in MCTS as compared to 2D cultures, as detected upon oligonucleotide array hybridization. **b**: Data are reported as mean fluorescence intensity (MFI) observed in cells from 2D or MCTS cultures upon staining with fluorochrome-labeled monoclonal antibodies (mAb) recognizing the indicated markers. MFI observed upon staining with isotype control mAbs were subtracted.

secretion of the corresponding proteins were also observed in these conditions. Indeed, IL-8 production was also detectable by immunohistochemistry in MCTS, mostly in inner cell layers.

There are no specific studies exploring the association between CCL20 gene expression and tumor progression in melanoma. However, in pancreatic cancers, tumorigenesis has been suggested to be associated with CCL20 gene expression (Kleeff et al., 1999). Furthermore, this chemokine has been suggested to favor the infiltration of melanoma by antigen presenting cells producing the immunosuppressive enzyme indoleamine 2,3-dioxygenase (IDO) (Lee et al., 2003).

In addition, notably, CXCL1, IL-8, and CCL20 are known to promote angiogenesis in vivo. Other genes whose products enhance angiogenesis, such as those encoding angiopoietin-like 4 and hypoxia-induced protein 2, were also overexpressed in MCTS. In striking contrast, however, basic FGF gene was downregulated in NA8 cells cultured in spheroids.

Genes encoding or regulating the production of ECM components, such as laminin or hyaluronic acid, were also upregulated together with the gene encoding CD54 (ICAM-1) in MCTS, as compared to monolayer cultures.

Taken together our data provide a first database focused on structure-related gene expression in tumor cells. Most importantly, they underline that the architecture of melanoma cells, possibly due to the inherent homotypic cell–cell interaction or specific microenvironmental conditions, with a putative role of hypoxia, may determine specific gene expression patterns of potentially high functional relevance. Strikingly, culture in MCTS appears to result in the upregulation of a constellation of genes whose expression has previously been shown to correlate with high malignancy.

The evaluation of the role of the third dimension, while adding to the complexity of model culture systems, might prove critical for the investigation of the tumor microenvironment including the interaction between tumor cells and autologous healthy cells with diverse physiological functions.

ACKNOWLEDGMENTS

This work was partially supported by grants from the Swiss National Science Foundation and by the Swiss Bridge Foundation to G.C.S.

LITERATURE CITED

Bajzer Z, Vuk-Pavlovic S, Huzak M. 1997. Mathematical modelling of tumor growth kinetics. In: Adam JA, Bellomo N editors. A survey of models for tumor-immune system dynamics. Boston: Birkhauser. pp 89–133.

Balentien E, Mufson BE, Shattuck RL, Derynck R, Richmond A. 1991. Effects of MGSA/GRO alpha on melanocyte transformation. Oncogene 6:1115–1124.

Bar-Eli M. 1999. Role of interleukin-8 in tumor growth and metastasis of human melanoma. Pathobiol 67:12–18.

Cavallaro U, Christofori G. 2004. Cell adhesion and signalling by cadherins and Ig-CAMS in cancer. Nat Rev Cancer 4:118–132.

Certa U, Seiler M, Padovan E, Spagnoli GC. 2001. High density oligonucleotide array analysis of interferon-α2a sensitivity and transcriptional response in melanoma cells. Br J Cancer 85:107–114.

Chignola R, Schenetti A, Andrighetto G, Chiesa E, Foroni R, Sartoris S, Tridente G, Liberati D. 2000. Forecasting the growth of multicell tumour spheroids: Implications for the dynamic growth of solid tumours. Cell Prolif 33:219–229.

Dangles V, Lazar V, Validire P, Richon S, Wertheimer M, Laville V, Janneau JL, Barrois M, Bovin C, Poynard T, Vallancien G, Bellet D. 2002. Gene expression profiles of bladder cancers: Evidence for a striking effect of in vitro cell models on gene patterns. Br J Cancer 86:1283–1289.

Dangles-Marie V, Richon S, El Behi M, Echchakir H, Dorothee G, Thiery J, Validire P, Vergnon I, Menez J, Ladjimi M, Chouaib S, Bellet D, Mami-Chouaib F. 2003. A three-dimensional tumor cell defect in activating autologous CTLs is associated with inefficient antigen presentation correlated with heat shock protein-70 down-regulation. Cancer Res 63:3682–3687.

Desoize B, Jardillier JC. 2000. Multicellular resistance: A paradigm for clinical resistance? Crit Rev Oncol Hematol 36:193–207.

Folkman J, Moscona A. 1978. Role of cell shape in growth control. Nature 273: 345–349.

Gervois N, Guilloux Y, Diez E, Jotereau F. 1996. Suboptimal activation of melanoma infiltrating lymphocytes (TIL) due to low avidity of TCR/MHC-tumor peptide interactions. J Exp Med 183:2403–2407.

Görlach A, Herter P, Hentschel H, Frosch PJ, Acker H. 1994. Effects of nIFNβ and rIFNγ on growth and morphology of two human melanoma cell lines: Comparison between two- and three-dimensional culture. Int J Cancer 56:249–254.

Hamid R, Rotshteyn Y, Rabadi L, Parikh R, Bullock P. 2004. Comparison of alamar blue and MTT assays for high throughput screening. Toxicol In Vitro 18:703–710.

Hauptmann S, Gebauer-Hartung P, Leclere A, Denkert C, Pest S, Losterhafen B, Dietel M. 1998. Induction of apoptosis in the centre of multicellular tumour spheroids of colorectal carcinoma—Involvement of CD95 pathway and differentiation. Apoptosis 3:267–279.

Kelm JM, Timmins NE, Brown CJ, Fussenegger M, Nielsen LK. 2003. Method for the generation of homogeneous multicellular tumor spheroids applicable to a wide variety of cell types. Biotechnol Bioeng 83:173–180.

Kleeff J, Kusama T, Rossi DL, Ishiwata T, Maruyama H, Friess H, Buchler MW, Zlotnik A, Kore M. 1999. Detection and localization of Mip-3alpha/LARC/Exodus, a macrophage proinflammatory chemokine, and its CCR6 receptor in human pancreatic cancer. Int J Cancer 81:650–657.

Koch AE, Polverini PJ, Kunkel SL, Harlow LA, DiPietro LA, Elner VM, Elner SG, Strieter RM. 1992. Interleukin-8 as a macrophage-derived mediator of angiogenesis. Science 258:1798–1801.

Lee JR, Dalton RR, Messina JL, Sharma MD, Smith DM, Burgess RE, Mazzella F, Antonia SJ, Mellor AL, Munn DH. 2003. Pattern of immunoregulatory antigen presenting cells in malignant melanoma. Lab Invest 83:1457–1466.

Luan J, Shattuck-Brandt R, Haghnegahdar H, Owen JD, Strieter R, Burdick M, Nirodi C, Beauchamp D, Johnson KN, Richmond A. 1997. Mechanism and biological significance of constitutive expression of MGSA/GRO chemokines in malignant melanoma tumor progression. J Leukoc Biol 62:588–597.

Ochsenbein AF, Sierro S, Odermatt B, Pericin M, Karrer U, Hermans J, Hemmi S, Hengartner H, Zinkernagel RM. 2001. Roles of tumor localization, second signals and cross priming in cytotoxic T-cell induction. Nature 411:1058–1064.

Oertli D, Marti WR, Zajac P, Noppen C, Kocher T, Padovan E, Adamina M, Schumacher R, Harder F, Heberer M, Spagnoli GC. 2002. Rapid induction of specific cytotoxic T lymphocytes against melanoma-associated antigens by a recombinant vaccinia virus vector expressing multiple immunodominant epitopes and costimulatory molecules in vivo. Hum Gene Ther 13:569–575.

Renkvist N, Castelli C, Robbins PF, Parmiani G. 2001. A listing of human tumor antigens recognized by T cells. Cancer Immunol Immunother 50:3–15.

Santini MT, Rainaldi G, Indovina PL. 1999. Multicellular tumour spheroids in radiation biology. Int J Radiat Biol 75:787–799.

Singh RK, Gutman M, Radinsky R, Bucana CD, Fidler IJ. 1994. Expression of interleukin-8 correlates with the metastatic potential of human melanoma cells in nude mice. Cancer Res 54:3242–3247.

Sutherland RM. 1988. Cell and environment interactions in tumor microregions: The multicell spheroid model. Science 240:177–184.

Weaver VM, Lelievre S, Lakins JN, Chrenek MA, Jones JCR, Giancotti F, Werb Z, Bissel MJ. 2002. B4 integrin-dependent formation of polarized three-dimensional architecture confers resistance to apoptosis in normal and malignant mammary epithelium. Cancer Cell 2:205–216.

Zajac P, Oertli D, Marti W, Adamina M, Bolli M, Gueller U, Noppen C, Padovan E, Schultz-Thater E, Heberer M, Spagnoli G. 2003. Phase I/II clinical trial of a non replicative vaccinia virus expressing multiple HLA-A0201 restricted tumor associated epitopes and costimulatory molecules in metastatic melanoma patients. Hum Gene Ther 14:1497–1510.